Accepted Manuscript

Dysregulated Gliotoxin Biosynthesis Attenuates the Production of Unrelated Biosynthetic Gene Cluster-Encoded Metabolites in *Aspergillus fumigatus*

Sean Doyle, Gary W. Jones, Stephen K. Dolan

PII: S1878-6146(17)30178-2

DOI: 10.1016/j.funbio.2017.12.007

Reference: FUNBIO 880

To appear in: *Fungal Biology*

Received Date: 21 July 2017

Revised Date: 20 November 2017

Accepted Date: 10 December 2017

Please cite this article as: Doyle, S., Jones, G.W., Dolan, S.K., Dysregulated Gliotoxin Biosynthesis Attenuates the Production of Unrelated Biosynthetic Gene Cluster-Encoded Metabolites in *Aspergillus fumigatus*, *Fungal Biology* (2018), doi: 10.1016/j.funbio.2017.12.007.

Running head: Biosynthetic Gene Cluster interactions.

Dysregulated Gliotoxin Biosynthesis Attenuates the Production of Unrelated Biosynthetic Gene Cluster-Encoded Metabolites in *Aspergillus fumigatus*.

Sean Doyle[a], Gary W. Jones[a,b] and Stephen K. Dolan[a,c*]

[a] Department of Biology, Maynooth University, Maynooth, Co. Kildare, Ireland.

[b] Current Affiliation: Centre for Biomedical Science Research, Leeds Beckett University, Leeds LS1 3HE, UK.

[c] Current Affiliation: Department of Biochemistry, University of Cambridge, Cambridge CB2 1QW, UK.

*** Corresponding Author:**

Dr Stephen K. Dolan, Department of Biochemistry, University of Cambridge, Cambridge CB2 1QW, UK.

Tel: 01223 (3)33640; Fax: 01223 333345 E-mail: skd41@cam.ac.uk

Keywords Methyltransferase, NRPS, fungal proteomics, LC-MS, metabolomics, BGC.

Abstract

Gliotoxin is an epipolythiodioxopiperazine (ETP) class toxin, contains a disulfide bridge that mediates its toxic effects via redox cycling and is produced by the opportunistic fungal pathogen *Aspergillus fumigatus*. The gliotoxin *bis*-thiomethyltransferase, GtmA, attenuates gliotoxin biosynthesis in *A. fumigatus* by conversion of dithiol gliotoxin to *bis*-thiomethylgliotoxin (BmGT). Here we show that disruption of dithiol gliotoxin *bis*-thiomethylation functionality in *A. fumigatus* results in significant remodelling of the *A. fumigatus* secondary metabolome upon extended culture. RP-HPLC and LC-MS/MS analysis revealed the reduced production of a plethora of unrelated biosynthetic gene cluster-encoded metabolites, including pseurotin A, fumagillin, fumitremorgin C and tryprostatin B, occurs in *A. fumigatus* Δ*gtmA* upon extended incubation. Parallel quantitative proteomic analysis of *A. fumigatus* wild-type and Δ*gtmA* during extended culture revealed cognate abundance alteration of proteins encoded by relevant biosynthetic gene clusters, allied to multiple alterations in hypoxia-related proteins. The data presented herein reveal a previously concealed functionality of GtmA in facilitating the biosynthesis of other BGC-encoded metabolites produced by *A. fumigatus*.

Introduction

Ascomycetes constitute the largest phylum of the fungal kingdom and produce an incredible array of natural products. Although many of these compounds are known as medicinal therapeutics or industrial chemicals, several natural products are potent toxins which pose substantial threats to human food supplies and health (Schueffler and Anke 2014). The opportunistic fungus *Aspergillus fumigatus* produces a wealth of these potent natural product toxins which are encoded by multigene biosynthetic gene clusters (BGCs) (Bignell *et al*. 2016).

Gliotoxin has been shown to be a virulence attribute in invasive aspergillosis due to its cytotoxic, genotoxic and apoptosis-stimulating properties. It is produced through a sequential series of enzymatic steps, which are predominantly encoded by the *gli* BGC (Dolan *et al*. 2015). Gliotoxin biosynthesis is also influenced by GtmA (TmtA in Scharf et al. (2014)), a thiol-directed methyltransferase encoded outside the *gli* BGC, which specifically *bis*-thiomethylates both thiols of dithiol gliotoxin to form *bis*-thiomethylgliotoxin (BmGT), resulting in the attenuation of gliotoxin formation (Dolan *et al*. 2014). Lines between defined BGCs have been blurred by elegant work describing the existence of intertwined biosynthetic gene clusters which are involved in the formation of more than one chemical product (Wiemann *et al*. 2013). For example, *A. fumigatus* encodes a "supercluster" in the subtelomeric region of chromosome 8, in which the genes responsible for the production of two natural products, pseurotin and fumagillin, are physically intertwined (Wiemann *et al*. 2013). Like gliotoxin, these other natural products also have potent toxicities. For example, pseurotin A is an immunosuppressive spirocyclic that has been shown to have interesting biological activities including the ability to induce the cellular differentiation of PC12 neuronal cells (Komagata *et al*. 1996), monoamine oxidase inhibitory activity (Maebayashi *et al*. 1985) and chitin synthase inhibitory activity (Wenke *et al*. 1993), highlighting many potential applications of this metabolite. Fumagillin has antibiotic and antifungal activity. It was also found to exhibit anti-cancer properties and anti-angiogenic activity as a inhibitor of the of the human type 2 methionine aminopeptidase (MetAP2) (Sin *et al*. 1997; Hou *et al*. 2009).

Despite the fact that BGCs often possess a pathway-specific transcription factor, the production of several otherwise unconnected natural products has been shown to be regulated by global regulators of secondary metabolism such as LaeA. This functionally enigmatic regulator has been shown to regulate the production of several *A. fumigatus* secondary metabolites (SMs) including gliotoxin, fumagillin, pseurotin A and helvolic acid (Perrin *et al*. 2007). LaeA has also been shown to counteract the establishment of heterochromatin marks, thus activating SM production, inferring that LaeA regulates BGC-encoded metabolism by modifying chromatin structure (Nützmann *et al*. 2011). This suggests that fungal SM is controlled by a rigorous hierarchy of regulatory mechanisms.

Understanding the diversity of regulatory strategies controlling the expression of these pathways is therefore critical if their biosynthetic potential is to be explored for new drug leads. No single medium under standardized growth conditions can secure expression of the full potential for producing the secondary metabolome of a fungal culture. However, there are many strategies to enable fungal cultures to produce even more BGC-encoded metabolites; for instance by modifying the media constituents, adding other microorganisms, using light or using longer incubation periods, alternate temperatures or deploying low or high pH (Ochi & Hosaka 2013).

The filamentous fungus *Aspergillus terreus* produces the ETP acetylaranotin (Guo et al. 2013). Similar to gliotoxin, this metabolite and its derivatives have been shown to display an array of interesting bioactivities including the induction of apoptosis in cancer cell lines and antifungal activity (Guo et al. 2013; Choi et al. 2011; Suzuki et al. 2000; Li et al. 2016). Three novel bis(methylthio)dioxopiperazine derivatives of the epipolythiodioxopiperazine (ETP) emestrin were produced by *Podospora australis* following static incubation of cultures at 23 °C for 14 days (Li *et al*. 2016). Like *P. australis*, *A. fumigatus* produces many thiomethylated forms of gliotoxin upon incubation for two weeks at 25 °C in the dark (Forseth *et al*. 2011). Extending the incubation duration of *A. terreus* cultures from 6 d to 42 d resulted in the production of four thiomethylated

forms of acetylaranotin, which were undetectable at earlier incubation time points. One of these bioactive SMs (bisdethiobis(methylsulfanyl)apoaranotin) exhibited growth inhibitory properties against *Mycobacterium tuberculosis* H37Ra with an MIC value of 1.56 µg/ml, thus highlighting the potential of extended incubation to develop exciting natural product derivatives (Haritakun *et al*. 2012). As the generation of these thiomethylated forms of acetylaranotin was likely dependent on an *A. terreus* GtmA homolog, this research prompted us to explore the effect of extended culture incubation on *A. fumigatus* wild-type and Δ*gtmA*. Moreover, despite significant work describing the production and isolation of these ETP derivatives (Dolan *et al*. 2014; Scharf *et al*. 2014; Liang *et al*. 2014), the downstream effects of removing this ETP *bis*-thiomethylation functionality and concomitant perpetuation of gliotoxin biosynthesis, have not been explored to date in extended cultures.

Materials and Methods

RP-HPLC and LC-MS detection of natural products from *A. fumigatus* culture supernatants

A. fumigatus wild-type, Δ*gtmA* and *gtmA*^{c} strains (Dolan et al. 2014) were grown (10^{8} conidia/ml) in quadruplicate (Czapek-Dox broth, 200 rpm, 3 d; then static, 25 d 37 °C). Culture supernatants and ethyl acetate organic extracts (100 μl) were analysed by RP-HPLC with UV detection (Agilent 1200 system), using a C18 RP-HPLC column (Agilent Zorbax Eclipse XDB-C18 Semi-Preparative; 5 μm particle size; 4.6 x 250 mm) at a flow rate of 2 ml/min (Figure 1). A mobile phase of water and acetonitrile with 0.1 % (v/v) trifluoroacetic acid, was used under various gradient conditions. For LC-MS analysis, organic extracts were diluted 1/10 in 0.1 % (v/v) formic acid and spin filtered prior to LC-MS analysis (Agilent Ion Trap 6340). Gliotoxin (purity: 98%) and BmGT (purity: 99%) standards were obtained from Sigma-Aldrich and Enzo Life Sciences, respectively. Fumagillin, pseurotin A, tryprostatin B and fumitremorgin C were identified based on published *m/z* ratios, retention times and fragmentation patterns as described previously (O'Keeffe *et al*. 2014). All data

were analysed using built-in GraphPad prism version 5.01 functions, as specified. The level of significance was set at $p < 0.05$ (*), $p < 0.001$ (**), and $p < 0.0001$ (***), unless otherwise stated.

Comparative quantitative proteomic analysis of *A. fumigatus* wild-type and mutant strains

As shown in Figure 1, Mycelia were then harvested and snap frozen in liquid N_2. No significant differnces in biomass were noted for these strains (Supplementary Figure 1 and 2). Mycelial lysates were prepared in lysis buffer (100 mM Tris-HCl, 50 mM NaCl, 20 mM EDTA, 10% (v/v) glycerol, 1 mM PMSF, 1 μg/ml pepstatin A, pH 7.5) with grinding, sonication and clarified using centrifugation. The resultant protein lysates were precipitated using trichloroacetic acid/acetone and resuspended in 100 mM Tris-HCl, 6 M urea, 2 M thiourea, pH 8.0. After dithiothreitol reduction and iodoacetamide-mediated alkylation, sequencing grade trypsin combined with ProteaseMax surfactant was added. All peptide mixtures were analysed via a Thermo Fisher Q-Exactive mass spectrometer coupled to a Dionex RSLCnano. LC gradients ran from 4-35 % B over 2 h, and data was collected using a Top15 method for MS/MS scans. Comparative proteome abundance and data analysis was performed using MaxQuant software (Version 1.3.0.5), with Andromeda used for database searching and Perseus used to organise the data (Version 1.4.1.3) (Cox & Mann 2008).

Results and Discussion

Late-stage culture metabolomics reveals that dysregulated gliotoxin biosynthesis due to *gtmA* absence influences the biosynthesis of other secondary metabolites

Comparative RP-HPLC analysis of culture supernatants at 3 d showed that the overall SM profile was not altered significantly by the deletion of *gtmA* (Figure 2A), except that gliotoxin production was significantly increased and *bis*-thiomethylgliotoxin (BmGT) production was abolished as described previously (Dolan *et al*. 2014). However, when the culture incubation time was increased by 25 d, a decrease in several compounds was specifically detected in *A.fumigatus* Δ*gtmA* by RP-HPLC DAD (at 254 nm and 351 nm) (Figure 2B,C). The production of these compounds was restored in the complemented strain (*gtmA*^{c}). These compounds were fraction-collected, analysed by

LC-MS and identities were elucidated based on known *m/z* values and fragmentation patterns. Pseurotin A (p =0.0001) and fumagillin (p = 0.0005) were produced at significantly decreased concentrations in *A. fumigatus* Δ*gtmA* (Figure 2D). Furthermore, LC-MS/MS analysis of ethyl-acetate extracted culture supernatants also uncovered that the detected concentration of tryprostatin B (p =0.0005) and fumitremorgin C (p =0.0074) were significantly lower in the Δ*gtmA* strain (Figure 2D). This suggested that GtmA activity may influence the production of other SM through the production of BmGT or, alternatively, by augmenting *gli*-cluster activity.

In order to uncover if the absence of BmGT was directly responsible for the metabolite alterations, the extended culture experiment was repeated and exogenous BmGT was added (10 μg/ml final) to *A. fumigatus* Δ*gtmA* prior to static incubation for 25 days (n = 4). Methanol was added to the control cultures. Exogenously added BmGT did not result in the restoration of pseurotin A or fumagillin production in *A. fumigatus* Δ*gtmA* to wild-type levels, suggesting that BmGT does not directly facilitate the production of these metabolites (Figure 2E).

Label-Free Quantitative (LFQ) proteomics of late-stage cultures reveals that the absence of *gtmA* expression and resulting dysregulated gliotoxin biosynthesis leads to widespread proteomic alterations

The metabolomic analysis demonstrated that *A. fumigatus* Δ*gtmA* has an altered SM profile in comparison with that of the wild-type or $gtmA^C$ cultured under identical conditions. Comparative label-free quantitative (LFQ) proteomic analysis was carried out to further elucidate the involvement of GtmA activity in this metabolite profile alteration. A total of 1468 proteins were detected in *A. fumigatus* wild-type vs. Δ*gtmA* analysis (Figure 3). Two proteins were uniquely detected in *A. fumigatus* Δ*gtmA* and 87 proteins were significantly more abundant in this mutant. Proteins (n =35) were not detected in *A. fumigatus* Δ*gtmA* and 136 proteins were significantly less abundant in this strain compared to wild-type. This dataset was cross referenced with the $gtmA^C$ vs. Δ*gtmA* dataset in order to confirm which of these changes were directly due to the absence of *gtmA*. Based on this enrichment, 27 proteins were not detected in *A. fumigatus* Δ*gtmA* and 93 proteins

were significantly less abundant in this strain. Two proteins were uniquely detected in *A. fumigatus* Δ*gtmA* under this condition and 71 proteins were significantly more abundant in this mutant (Table S1 and S2).

Four proteins encoded by the *gli* cluster were shown to be significantly more abundant (log2-fold) in Δ*gtmA* compared to the wild-type. The MFS gliotoxin efflux transporter GliA (AFUA_6G09710; 1.82652), the membrane dipeptidase GliJ (AFUA_6G09650; 1.66652), a predicted *O*-methyltransferase GliM (AFUA_6G09680; 1.62724) and the glutathione *S*-transferase GliG (AFUA_6G09690; 1.40425) were increased in abundance in Δ*gtmA* (Table S1). Additionally, a putative short chain dehydrogenase (AFUA_4G08710; 1.37478) and a ThiJ/PfpI family protein (AFUA_5G01430; 1.93416), which were previously shown to be induced by gliotoxin exposure were more abundant in this condition. RmtA (AFUA_1G06190; 1.06), a putative arginine methyltransferase previously shown to act as a global regulator in *A. flavus*, mediating broad effects on secondary metabolism and development in this organism (Satterlee *et al*. 2016), also exhibited significantly elevated abundance. However, its role in *A. fumigatus* has yet to be elucidated.

Co-incident with the reduced levels of selected SMs, several proteins for which cognate transcripts have previously been shown to be induced by hypoxia, or by exposure to neutrophils, were increased in abundance in *A. fumigatus* Δ*gtmA*. Two proteins which are repressed by gliotoxin exposure and two which are repressed by hypoxia (Vödisch *et al*. 2011) were significantly decreased in abundance in Δ*gtmA*. This may be a response to the sustained gliotoxin production in *A. fumigatus* Δ*gtmA* as the abundance of these proteins is returned to wild-type levels in the complemented strain. Proteins which had been shown previously to be induced by hypoxia exposure were significantly more abundant in *A. fumigatus* Δ*gtmA* compared to the wild-type (Vödisch *et al*. 2011). These include a putative transaldolase (AFUA_5G09230; 1.58072), a putative glyceraldehyde 3-phosphate dehydrogenase (AFUA_5G01030; 1.34405), an argininosuccinate lyase (AFUA_3G07790; 1.34137), a 6-phosphogluconate dehydrogenase (AFUA_6G08050; 1.31184), a putative mevalonate kinase (AFUA_4G07780; 1.07826), and an

essential 1, 3-beta-glucanosyltransferase (AFUA_2G05340; 1.0025). Additionally, glutathione synthase (AFUA_5G06610; 1.67077), which is an ortholog of the *Saccharomyces cerevisiae* GSH2 glutathione biosynthetic protein, known to be induced by oxidative stress in this organism (Sugiyama *et al*. 2000), was more abundant. Additionally, proteins formerly shown to be induced by neutrophil exposure were also more abundant in Δ*gtmA* (Sugui *et al*. 2008). These included a putative carbon-nitrogen family hydrolase (AFUA_5G02350; 1.567), a putative myo-inositol-phosphate synthase (AFUA_2G01010; 1.21826) and an aldehyde reductase (AKR1) (AFUA_6G10260; 1.09358). Mannitol 2-dehydrogenase which has a predicted role in mannitol metabolism (AFUA_4G14450; 1.52766) was also more abundant. Mannitol is an important virulence determinant of pathogenic fungi. Its high antioxidant capacity aids in suppressing the reactive oxygen species mediated attacks from neutrophils (Wyatt *et al*. 2014). This suggests that the sustained expression of the *gli*-cluster in long-term cultures may be translated as an oxidative challenge to *A. fumigatus*.

Six transporter proteins were found to be significantly more abundant in Δ*gtmA*. These were an ABC transporter Cdr1B (AFUA_1G14330; 2.4345), a putative MFS monocarboxylate transporter (AFUA_3G03320; 2.29482) (located in an uncharacterised SM cluster (Lind *et al*. 2016), the ABC multidrug transporter Mdr1 (AFUA_5G06070; 2.19999), a putative plasma membrane H^+ ATPase Pma1 (AFUA_3G07640; 1.3888), the low affinity plasma membrane zinc transporter ZrfB (AFUA_2G03860; 1.30673), which is induced by zinc depletion and the amino acid permease Gap1 (AFUA_7G04290; 1.0342). Pma1 was upregulated during conidial germination and in response to amphotericin B and downregulated by caspofungin treatment (Gautam *et al*. 2008; Cagas *et al*. 2011). Overexpression of the Cdr1B transporter was reported to be responsible for azole resistance in a clinical setting (Fraczek *et al*. 2013). The Zn_2-Cys_6 transcription factor AtrR was recently shown to be responsible for regulating cdr1B expression in *A. fumigatus* (Hagiwara *et al*. 2017).

Aminoacyl-tRNA synthetases are central enzymes in translation which provide the charged tRNAs needed for protein synthesis (Guo *et al*. 2010). Tyrosyl-tRNA synthetase (AFUA_5G10640; 2.85558), Seryl-tRNA synthetase (AFUA_5G05490; 1.22428), Putative valyl-tRNA synthetase (AFUA_8G04800; 1.22314), Isoleucyl-tRNA synthetase (AFUA_1G13710; 1.10632) and a putative Lysyl-tRNA synthetase (AFUA_6G07640; 1.05645) were significantly more abundant in *A. fumigatus* Δ*gtmA* compared to the wild-type. Several cell wall-related proteins were increased in abundance in *A. fumigatus* Δ*gtmA*. These included the GPI-anchored cell wall beta-1,3-endoglucanase Bgt2 (AFUA_3G00270; 1.35218) and three β(1-3)glucanosyltransferases which belong to the 7-member GEL family (Fontaine *et al*. 2003; Gastebois *et al*. 2010); Gel5 (AFUA_8G02130; 1.23988), Gel3 (AFUA_2G12850; 1.00391), and Gel4 (AFUA_2G05340; 1.0025; previously shown to be increased in hypoxia). GlfA, a UDP-galactopyranose mutase (AFUA_3G12690; 1.3312), was also significantly more abundant. *A. fumigatus* Δ*glfA* is devoid of galactofuranose and displays attenuated virulence in a low-dose mouse model of invasive aspergillosis (Schmalhorst *et al*. 2008). Interestingly, the small monomeric GTPase RasA (AFUA_5G11230; 1.65165) was also significantly more abundant in Δ*gtmA*. A Δ*rasA* mutant demonstrated a phenotype of cell wall instability and slow germination (Fortwendel *et al*. 2008). Higher levels of RasA abundance may be linked to the cell wall remodelling described above.

As mentioned above, *A. fumigatus* Δ*gtmA* 28 d cultures showed a significant decrease in the production of pseurotin A and fumagillin compared to the wild-type strain. Complementary LFQ proteomic analysis revealed a significant decrease in abundance of several proteins encoded by the chromosome 8 supercluster (AFUA_8G00100-00720) (Wiemann *et al*. 2013), in agreement with the metabolomic analysis which revealed the decreased production of pseurotin A and fumagillin (Figure 4). A total of 15 proteins from this cluster were detected as less abundant in Δ*gtmA*. Interestingly, 19 of the 98 proteins detected as significantly decreased in abundance in Δ*gtmA* are encoded on Chromosome 8, whereas 2 of the 38 proteins which were detected as increased in abundance in Δ*gtmA* were similarly located. O'Keeffe et al. (2014) demonstrated that an intact

gliotoxin self-protection mechanism, mediated by GliT, is essential to regulate the biosynthesis of apparently unrelated metabolites such as pseurotin A, fumagillin and fumitremorgins. Herein, we have shown that when *A. fumigatus* cultures are incubated for extended duration, the absence of GtmA, resulting in dysregulated gliotoxin production, also has downstream effects on the biosynthesis of apparently unrelated natural products produced by this organism. A total of 17 proteins from the supercluster (Wiemann et al. 2013) were detected as less abundant in Δ*gtmA*. Interestingly, 23 of the 136 proteins detected as significantly decreased in abundance in Δ*gtmA* are encoded on Chromosome 8. This is in comparison to 2 of the 72 proteins detected as increased in abundance in Δ*gtmA* being encoded on Chromosome 8. Several proteins encoded by the supercluster were either undetectable or significantly decreased in abundance in *A. fumigatus* Δ*gtmA* (Table 3; Table S2). Four proteins involved in the synthesis of fumitremorgins were significantly decreased in abundance in Δ*gtmA*. FtmPT1 (AFUA_8G00210; not detected) and FtmPT2 (AFUA_8G00250; not detected), two prenyltransferases involved in fumitremorgin B biosynthesis, FtmD, an *O*-methyltransferase involved in fumitremorgin B synthesis (AFUA_8G00200; not detected), and FtmF, an alpha-ketoglutarate-dependent dioxygenase which catalyses the conversion of fumitremorgin B to verruculogen (AFUA_8G00230; -4.32466). Six proteins associated with fumagillin biosynthesis were not detected or significantly less abundant. These were the fumagillin polyketide synthase (Fma-PKS) (AFUA_8G00370; not detected), the fumagillin phytanoyl-CoA-oxidase FmaF (AFUA_8G00480; -4.17772), FmaD, the fumagillin *O*-methyltransferase (AFUA_8G00390; -3.85167), a hypoxia induced protein; encoded in the fma gene cluster (AFUA_8G00430; -3.24847), FmaC, a putative fumagillin alpha/beta hydrolase (AFUA_8G00380; -3.16375) and a putative *O*-methyltransferase; encoded in the *fma* gene cluster (AFUA_8G00400; -2.85247). Four proteins involved in pseurotin A biosynthesis were significantly less abundant. PsoB, PsoD, PsoC, a putative pseurotin A methyltransferase (AFUA_8G00550; -3.28917), PsoA, the pseurotin A non-ribosomal peptide synthetase (AFUA_8G00540; -1.60039), a pseurotin A dual-functional mono- oxygenase/methyltransferase PsoE (AFUA_8G00560; not

detected) and PsoF, a putative pseurotin A dual methyltransferase/monooxygenase (AFUA_8G00440; -2.74114) (Table 3; Table S2). A glutathione S-transferase (AFUA_4G14380; -2.96915) encoded within the helvolic acid cluster (AFUA_4G14380–4850) (Mitsuguchi et al. 2009) was also decreased in abundance in *A. fumigatus* Δ*gtmA*.

Two proteins shown previously to be repressed by gliotoxin exposure (Carberry et al. 2012) were shown to be significantly decreased in abundance in Δ*gtmA*: a mitochondrial peroxiredoxin (AFUA_4G08580; -1.96889) with a predicted role in cell redox homeostasis regulation and a putative alcohol dehydrogenase (AFUA_7G01000; -1.17862) involved in ethanol metabolism. A putative thioredoxin (AFUA_8G01090; not detected) and an M repeat protein (AFUA_6G08660; -1.99673), which were shown to be hypoxia-repressed were also decreased in expression (Vödisch *et al*. 2011) (Table S2). The thiol methyltransferase GtmA (Dolan et al. 2014 & 2017) was uniquely detected in the wild-type condition and abundance was restored in the complemented strain. Several cell wall associated proteins were also not detected or decreased in abundance in *A. fumigatus* Δ*gtmA* mutant in comparison with the wild-type. These included the conidial hydrophobin RodA (AFUA_5G09580; not detected), a putative glycophosphatidylinositol (GPI)-anchored cell wall protein MP-2 (AFUA_2G05150; not detected) and a putative phiA family cell wall protein (AFUA_3G03060; -1.5461).

Several mitochondrial-associated proteins were not detected or less abundant in Δ*gtmA*. These included an uncharacterized protein (AFUA_1G13195; not detected) with orthologs involved in cristae formation and integral to mitochondrial inner membrane, a putative iron-sulfur cluster biosynthesis protein extrinsic to mitochondrial inner membrane (AFUA_3G06492, not detected), a putative mitochondrial intermembrane space translocase subunit (AFUA_1G04470; 1.97737), a putative mitochondrial peroxiredoxin (AFUA_4G08580; -1.96889) with a predicted role in cell redox homeostasis regulation, a putative prohibitin (AFUA_2G09090; -1.5947) with orthologs involved in mitochondrion inheritance, a putative mitochondrial 2-oxodicarboxylate carrier protein

(AFUA_1G09660; -1.56908), a putative adenylate kinase with mitochondrial intermembrane space localization (AFUA_1G07530; -1.4474), a putative outer mitochondrial membrane protein porin (AFUA_4G06910; -1.31711), a putative mitochondrial genome maintenance protein Mgm101 (AFUA_2G09560; 1.26767), a mitochondrial glycerol-3-phosphate dehydrogenase (AFUA_1G08810; -1.19813) and a putative mitochondrial processing peptidase alpha subunit with a role in protein processing involved in protein targeting to mitochondrion (AFUA_1G11870; -1.1768). Interestingly, several hypoxia-induced proteins were either not detected or decreased in abundance in *A. fumigatus* Δ*gtmA* (Blatzer *et al*. 2011). These included a gamma-glutamyltranspeptidase (AFUA_4G13580, not detected); SrbA-regulated during hypoxia, Putative flavohemoprotein (AFUA_4G03410; -1.42304), Putative outer mitochondrial membrane protein porin (AFUA_4G06910; -1.31711), Ubiquinol-cytochrome c reductase iron-sulphur subunit precursor (AFUA_5G10610; -1.19224) with a predicted role in oxidative phosphorylation, an aspartic acid endopeptidase (AFUA_3G11400; -1.18445) and a thiamine biosynthesis protein (AFUA_5G02470; -1.11766).

Gliotoxin can act as a sporulation signal for *A. nidulans* development under mildly reducing conditions through NapA oxidative stress regulation, as reflected by green conidial pigmentation (Zheng *et al*. 2015). Altough no phenotypic differences were noted for Δ*gtmA*, it is conceivable that the absence of gliotoxin *bis*-thiomethylation can alter the normal course of fungal development by sustaining the *gli*-cluster activation signal. It is speculated that this may then lead to downstream redox stress signalling, cell wall remodelling and the modification of secondary metabolite profiles.

Conclusions

Overall these data show that the loss of GtmA-mediated thiomethylation upon extended culture duration has downstream effects on seemingly unrelated BGC-encoded metabolites in *A. fumigatus*. The exact mechanism of this effect is unclear, however, it is likely that the sustained *gli*-cluster activation in the absence of GtmA artificially prioritises the expression of this cluster,

resulting in extensive downstream proteomic remodelling, which occurs at the expense of other BGCs in this organism. We also explored the possiblilty that BmGT itself acts as a signal to sustain the expression of the unrelated BGC-encoded metabolites, which decrease in its absence. Adding a high concentration (10 μg/mL) of BmGT to the cultures did not complement the phenotype, suggesting that BmGT itself does not sustain the expression of these unrelated clusters. It's important to note that although *A. fumigatus* exposure to GT results in a rapid intracellular accumulation due to the redox properties of this metabolite (Bernardo *et al*. 2003), BmGT does not have this capability due to the absence of the characteristic disulfide bridge. This means that we cannot completely rule out that the intracellular accumulation of BmGT is responsible this phenotype. However, as shown in our earlier study, exposure of *A. fumigatus* to 5 µg/ml BmGT results in a distinct proteomic response, increasing the GliT and GtmA protein abundance 2 fold (Dolan *et al*. 2014). This would suggest that despite its inability to accumulate intracellularly to the same extent as GT, exogenously added BmGT can act as a signalling molecule in *A. fumigatus* when applied exogenously.

Although several master regulators have been shown to orchestrate secondary metabolism in fungi, this work highlights the importance of the BGC-encoded metabolites themselves as important signals in rewiring SM production. Despite our extensive functional and mechanistic insight into how these BGC-encoded metabolites are synthesised, the precise mechanism of how intracellular signals orchestrate temporal control over SM production have yet to be understood. Further work will focus on the precise nature of how exactly these competing metabolic signals are integrated, resulting in the expression of a 'typical' secondary metabolome of *A. fumigatus* and other pathogenic fungi.

Acknowledgements

This work was funded by a Science Foundation Ireland Principal Investigator Award to SD (PI/11/1188). SKD was a recipient of an Irish Research Council Embark PhD Fellowship. LC-MS

345 facilities were funded by competitive awards from Science Foundation Ireland (12/RI/2346 (3)) and
346 the Irish Higher Education Authority.

347 **Figure 1**. Flow diagram describing the experimental setup. Wild-type, Δ*gtmA* and *gtmA*^{C} were
348 grown for 3 d shaking at 37° C. Cultures where then incubated at 37 °C, static for a further 25 d.
349 Culture supernatants were analysed by RP-HPLC at 3 d, Samples were analysed by RP-HPLC, LC-
350 MS/MS and quantitative proteomics at 28 d.

351 **Figure 2. A.** RP-HPLC analysis of *A. fumigatus* wild-type, Δ*gtmA* and *gtmA*^{C} culture supernatants
352 at 72 h. No alteration of the secondary metabolite profile was altered, except the absence of BmGT
353 and increase in GT due to the absence of *gtmA*. **B./C.** RP-HPLC analysis of *A. fumigatus* WT,
354 Δ*gtmA* and *gtmA*^{C} culture supernatants at 28 d. Major alterations in the SM profile are evident,
355 notably at 254 nm and 351 nm. The abundance of the compounds pseurotin A and fumagillin were
356 significantly reduced in the Δ*gtmA* strain. **D.** LC-MS/MS analysis of organically extracted culture
357 supernatants of *A. fumigatus* wild-type, Δ*gtmA* and *gtmA*^{C} culture supernatants at 28 d. Pseurotin A,
358 fumagillin, tryprostatin B and fumitremorgin C were detected at significantly reduced levels in
359 Δ*gtmA*. **E.** Exogenous addition of methanol or BmGT (10 μg/ml) to Δ*gtmA* (quadruplicate) prior to
360 static incubation for 25 d did not result in the restoration of pseurotin A or fumagillin production
361 levels to that of the wild-type strain. Bars represent pseurotin A or fumagillin RP-HPLC intensity
362 (mAU) at 254 nm.

363 **Figure 3.** Venn-diagram illustrating the proteins with altered abundance in *A. fumigatus* wild-type
364 when compared to Δ*gtmA*. Heat map depicting hierarchal clustered expression data of the 260
365 proteins of differential abundance in Δ*gtmA* compared to the wild-type.

366 **Figure 4.** Absence of GtmA during long-term incubation of *A. fumigatus* results in the increased
367 expression of the *gli*-cluster, widespread proteomic alterations and the decreased abundance of
368 BGC-encoded enzymes located on chromosome 8. This in turn results in the reduced production of
369 the respective compounds.

Table 1: Top 10 proteins with increased abundance in *A. fumigatus* Δ*gtmA* compared to wild-type following extended culture. Data sorted by fold change, in descending order.

Table 2: Top 10 proteins with decreased abundance in *A. fumigatus* Δ*gtmA* compared to wild-type following extended culture. Data sorted by fold change, in descending order.

Table 3: Proteins encoded by the intertwined secondary metabolite supercluster on chromosome 8 of *A. fumigatus* (AFUA_8G00100-00720) with **decreased** abundance in *A. fumigatus* Δ*gtmA* compared to wild-type and *gtmA*^{c} grown for 28 days in Czapek-Dox media. Data sorted by fold change, in descending order.

Supplementary Figure 1: Image of *A. fumigatus* wild-type and Δ*gtmA* long term incubation cultures immediately prior to harvesting.

Supplementary Figure 2: Calculated mycelial dry weight from snap frozen, lyophilised mycelia for *A. fumigatus* wild-type, Δ*gtmA* and *gtmA*C following long term incubation.

References

Bernardo PH, Brasch N, Chai CLL, Waring P, 2003. A Novel Redox Mechanism for the Glutathione-dependent Reversible Uptake of a Fungal Toxin in Cells. *Journal of Biological Chemistry* **278**: 46549–46555. https://doi.org/10.1074/jbc.M304825200

Bignell E, Cairns TC, Throckmorton K, Nierman WC, Keller NP, 2016. Secondary metabolite arsenal of an opportunistic pathogenic fungus. *Philosophical Transactions of the Royal Society of London B: Biological Sciences* **371**.

Blatzer M, Barker BM, Willger SD, Beckmann N, Blosser SJ, Cornish EJ, Mazurie A, Grahl N, Haas H, Cramer RA, 2011. SREBP coordinates iron and ergosterol homeostasis to mediate triazole drug and hypoxia responses in the human fungal pathogen Aspergillus fumigatus. *PLoS genetics* **7**: e1002374. https://doi.org/10.1371/journal.pgen.1002374

Cagas SE, Jain R, Li H, Perlin DS, 2011. Profiling the Aspergillus fumigatus Proteome in Response to Caspofungin. *ANTIMICROBIAL AGENTS AND CHEMOTHERAPY* **55**: 146–154. https://doi.org/10.1128/AAC.00884-10

Choi EJ, Park J-S, Kim Y-J, Jung J-H, Lee JK, Kwon HC, Yang HO, 2011. Apoptosis-inducing effect of diketopiperazine disulfides produced by Aspergillus sp. KMD 901 isolated from marine sediment on HCT116 colon cancer cell lines. *Journal of applied microbiology* **110**: 304–13. https://doi.org/10.1111/j.1365-2672.2010.04885.x

Cox J, Mann M, 2008. MaxQuant enables high peptide identification rates, individualized p.p.b.-range mass accuracies and proteome-wide protein quantification. *Nature biotechnology* **26**: 1367–72. https://doi.org/10.1038/nbt.1511

Dolan SK, O'Keeffe G, Jones GW, Doyle S, 2015. Resistance is not futile: Gliotoxin biosynthesis, functionality and utility. *Trends in Microbiology*: 1–10. https://doi.org/10.1016/j.tim.2015.02.005

Dolan SK, Owens RA, O'Keeffe G, Hammel S, Fitzpatrick DA, Jones GW, Doyle S, 2014. Regulation of nonribosomal peptide synthesis: bis-thiomethylation attenuates gliotoxin biosynthesis in Aspergillus fumigatus. *Chemistry & biology* **21**: 999–1012. https://doi.org/10.1016/j.chembiol.2014.07.006

Fontaine T, Magnin T, Melhert A, Lamont D, Latg?? JP, Ferguson MAJ, 2003. Structures of the glycosylphosphatidylinositol membrane anchors from Aspergillus fumigatus membrane

proteins. *Glycobiology* **13**: 169–177. https://doi.org/10.1093/glycob/cwg004

Forseth RR, Fox EM, Chung D, Howlett BJ, Keller NP, Schroeder FC, 2011. Identification of cryptic products of the gliotoxin gene cluster using NMR-based comparative metabolomics and a model for gliotoxin biosynthesis. *Journal of the American Chemical Society* **133**: 9678–9681. https://doi.org/10.1021/ja2029987

Fortwendel JR, Fuller KK, Stephens TJ, Bacon WC, Askew DS, Rhodes JC, 2008. Aspergillus fumigatus RasA regulates asexual development and cell wall integrity. *Eukaryotic cell* **7**: 1530–9. https://doi.org/10.1128/EC.00080-08

Fraczek MG, Bromley M, Buied A, Moore CB, Rajendran R, Rautemaa R, Ramage G, Denning DW, Bowyer P, 2013. The cdr1B efflux transporter is associated with non-cyp51a-mediated itraconazole resistance in Aspergillus fumigatus. *Journal of Antimicrobial Chemotherapy* **68**: 1486–1496. https://doi.org/10.1093/jac/dkt075

Gastebois A, Fontaine T, Latgé J-P, Mouyna I, 2010. beta(1-3)Glucanosyltransferase Gel4p is essential for Aspergillus fumigatus. *Eukaryotic cell* **9**: 1294–8. https://doi.org/10.1128/EC.00107-10

Gautam P, Shankar J, Madan T, Sirdeshmukh R, Sundaram CS, Gade WN, Basir SF, Sarma PU, 2008. Proteomic and transcriptomic analysis of Aspergillus fumigatus on exposure to amphotericin B. *Antimicrobial agents and chemotherapy* **52**: 4220–7. https://doi.org/10.1128/AAC.01431-07

Guo M, Yang X-L, Schimmel P, 2010. New functions of aminoacyl-tRNA synthetases beyond translation. *Nature reviews. Molecular cell biology* **11**: 668–74. https://doi.org/10.1038/nrm2956

Guo C-J, Yeh H-H, Chiang Y-M, Sanchez JF, Chang S-L, Bruno KS, Wang CCC, 2013. Biosynthetic pathway for the epipolythiodioxopiperazine acetylaranotin in Aspergillus terreus revealed by genome-based deletion analysis. *Journal of the American Chemical Society* **135**: 7205–13. https://doi.org/10.1021/ja3123653

Hagiwara D, Miura D, Shimizu K, Paul S, Ohba A, Gonoi T, Watanabe A, Kamei K, Shintani T, Moye-Rowley WS, Kawamoto S, Gomi K, 2017. A Novel Zn 2 -Cys 6 Transcription Factor AtrR Plays a Key Role in an Azole Resistance Mechanism of Aspergillus fumigatus by Co-regulating cyp51A and cdr1B Expressions. https://doi.org/10.1371/journal.ppat.1006096

Haritakun R, Rachtawee P, Komwijit S, Nithithanasilp S, Isaka M, 2012. Highly conjugated ergostane-type steroids and aranotin-type diketopiperazines from the fungus Aspergillus terreus BCC 4651. *Helvetica Chimica Acta* **95**: 308–313. https://doi.org/10.1002/hlca.201100335

Hou L, Mori D, Takase Y, Meihua P, Kai K, Tokunaga O, 2009. Fumagillin inhibits colorectal cancer growth and metastasis in mice: *In vivo* and *in vitro* study of anti-angiogenesis. *Pathology International* **59**: 448–461. https://doi.org/10.1111/j.1440-1827.2009.02393.x

Komagata D, Fujita S, Yamashita N, Saito S, Morino T, 1996. Novel neuritogenic activities of pseurotin A and penicillic acid. *The Journal of antibiotics* **49**: 958–9.

Liang W-L, Le X, Li H-J, Yang X-L, Chen J-X, Xu J, Liu H-L, Wang L-Y, Wang K-T, Hu K-C, Yang D-P, Lan W-J, 2014. Exploring the Chemodiversity and Biological Activities of the Secondary Metabolites from the Marine Fungus Neosartorya pseudofischeri. *Marine Drugs* **12**: 5657–5676. https://doi.org/10.3390/md12115657

Li Y, Yue Q, Krausert NM, An Z, Gloer JB, Bills GF, 2016. Emestrins: Anti- *Cryptococcus* Epipolythiodioxopiperazines from *Podospora australis*. *Journal of Natural Products* **79**: 2357–2363. https://doi.org/10.1021/acs.jnatprod.6b00498

Lind AL, Smith TD, Saterlee T, Calvo AM, Rokas A, 2016. Regulation of Secondary Metabolism by the Velvet Complex Is Temperature-Responsive in Aspergillus. *G3 (Bethesda, Md.)* **6**: 4023–4033. https://doi.org/10.1534/g3.116.033084

Maebayashi Y, Horie Y, Satoh Y, Yamazaki M, 1985. Isolation of pseurotin A and a new pyrazine from Pseudallescheria boydii. *Mycotoxins* **1985**: 33–34.

https://doi.org/10.2520/myco1975.1985.22_33

Nützmann H-W, Reyes-Dominguez Y, Scherlach K, Schroeckh V, Horn F, Gacek A, Schümann J, Hertweck C, Strauss J, Brakhage AA, 2011. Bacteria-induced natural product formation in the fungus Aspergillus nidulans requires Saga/Ada-mediated histone acetylation. *Proceedings of the National Academy of Sciences of the United States of America* **108**: 14282–7. https://doi.org/10.1073/pnas.1103523108

O'Keeffe G, Hammel S, Owens R a, Keane TM, Fitzpatrick D a, Jones GW, Doyle S, 2014. RNA-seq reveals the pan-transcriptomic impact of attenuating the gliotoxin self-protection mechanism in Aspergillus fumigatus. *BMC genomics* **15**: 894. https://doi.org/10.1186/1471-2164-15-894

Ochi K, Hosaka T, 2013. New strategies for drug discovery: activation of silent or weakly expressed microbial gene clusters. *Applied Microbiology and Biotechnology* **97**: 87–98. https://doi.org/10.1007/s00253-012-4551-9

Perrin RM, Fedorova ND, Jin WB, Cramer RA, Wortman JR, Kim HS, Nierman WC, Keller NP, 2007. Transcriptional regulation of chemical diversity in Aspergillus fumigatus by LaeA. *PLoS Pathogens* **3**: 508–517. https://doi.org/10.1371/journal.ppat.0030050

Satterlee T, Cary JW, Calvo AM, 2016. RmtA, a Putative Arginine Methyltransferase, Regulates Secondary Metabolism and Development in Aspergillus flavus (GH Goldman, Ed,). *PLOS ONE* **11**: e0155575. https://doi.org/10.1371/journal.pone.0155575

Scharf DH, Habel A, Heinekamp T, Brakhage AA, Hertweck C, 2014. Opposed effects of enzymatic gliotoxin N - And S -methylations. *Journal of the American Chemical Society* **136**: 11674–11679. https://doi.org/10.1021/ja5033106

Schmalhorst PS, Krappmann S, Vervecken W, Rohde M, Müller M, Braus GH, Contreras R, Braun A, Bakker H, Routier FH, 2008. Contribution of galactofuranose to the virulence of the opportunistic pathogen Aspergillus fumigatus. *Eukaryotic cell* **7**: 1268–77. https://doi.org/10.1128/EC.00109-08

Schueffler A, Anke T, 2014. Fungal natural products in research and development. *Natural Product Reports*: 1425–1448. https://doi.org/10.1039/C4NP00060A

Sin N, Meng L, Wang MQ, Wen JJ, Bornmann WG, Crews CM, 1997. The anti-angiogenic agent fumagillin covalently binds and inhibits the methionine aminopeptidase, MetAP-2. *Proceedings of the National Academy of Sciences of the United States of America* **94**: 6099–103.

Sugiyama K, Izawa S, Inoue Y, 2000. The Yap1p-dependent induction of glutathione synthesis in heat shock response of Saccharomyces cerevisiae. *The Journal of biological chemistry* **275**: 15535–40.

Sugui JA, Kim HS, Zarember KA, Chang YC, Gallin JI, Nierman WC, Kwon-Chung KJ, 2008. Genes differentially expressed in conidia and hyphae of Aspergillus fumigatus upon exposure to human neutrophils. *PloS one* **3**: e2655. https://doi.org/10.1371/journal.pone.0002655

Suzuki Y, Takahashi H, Esumi Y, Arie T, Morita T, Koshino H, Uzawa J, Uramoto M, Yamaguchi I, 2000. Haematocin, a new antifungal diketopiperazine produced by Nectria haematococca Berk. et Br. (880701a-1) causing nectria blight disease on ornamental plants. *The Journal of antibiotics* **53**: 45–9.

Vödisch M, Scherlach K, Winkler R, Hertweck C, Braun H-P, Roth M, Haas H, Werner ER, Brakhage AA, Kniemeyer O, 2011. Analysis of the *Aspergillus fumigatus* Proteome Reveals Metabolic Changes and the Activation of the Pseurotin A Biosynthesis Gene Cluster in Response to Hypoxia. *Journal of Proteome Research* **10**: 2508–2524. https://doi.org/10.1021/pr1012812

Wenke J, Anke H, Sterner O, 1993. Pseurotin A and 8- *O* -Demethylpseurotin A from *Aspergillus fumigatus* and Their Inhibitory Activities on Chitin Synthase. *Bioscience, Biotechnology, and Biochemistry* **57**: 961–964. https://doi.org/10.1271/bbb.57.961

Wiemann P, Guo C-J, Palmer JM, Sekonyela R, Wang CCC, Keller NP, 2013. Prototype of an

519 intertwined secondary-metabolite supercluster. *Proceedings of the National Academy of*
520 *Sciences of the United States of America* **110**: 17065–70.
521 https://doi.org/10.1073/pnas.1313258110
522 Wyatt TT, van Leeuwen MR, Wösten HAB, Dijksterhuis J, 2014. Mannitol is essential for the
523 development of stress-resistant ascospores in Neosartorya fischeri (Aspergillus fischeri).
524 *Fungal genetics and biology : FG & B* **64**: 11–24. https://doi.org/10.1016/j.fgb.2013.12.010
525 Zheng H, Kim J, Liew M, Yan JK, Herrera O, Bok JW, Kelleher NL, Keller NP, Wang Y, 2015.
526 Redox metabolites signal polymicrobial biofilm development via the NapA oxidative stress
527 cascade in Aspergillus. *Current biology : CB* **25**: 29–37.
528 https://doi.org/10.1016/j.cub.2014.11.018
529

Table 1: Top 10 proteins with increased abundance in *A. fumigatus* Δ*gtmA* compared to wild-type following extended culture. Data sorted by fold change, in descending order.

Protein Description	Log_2(Fold Increase)	Peptides	Seq coverage [%]	Protein IDs
Aldo-keto reductase. In uncharacterised secondary metabolite cluster.	2.85624	9	36.2	AFUA_2G01410
Tyrosyl-tRNA synthetase, cytoplasm, nucleus localization	2.85558	10	34.5	AFUA_5G10640
ABC transporter; Cdr1B, mutation causes increased azole sensitivity	2.4345	18	16.2	AFUA_1G14330
MFS monocarboxylate transporter, putative	2.29482	2	4.5	AFUA_3G03320
ABC multidrug transporter Mdr1	2.19999	25	25	AFUA_5G06070
Aminotransferase family protein, putative	2.09468	12	38	AFUA_2G13295
Glycerate dehydrogenase	2.01153	7	28	AFUA_1G13630
ThiJ/PfpI family protein; abundant in conidia	1.93416	9	55.1	AFUA_5G01430
Glutamyl-tRNA(Gln) amidotransferase, subunit A	1.93045	12	34.5	AFUB_092380
MFS gliotoxin efflux transporter GliA, encoded in the gliotoxin biosynthetic gene cluster	1.82652	4	9.2	AFUA_6G09710

Table 2: Top 10 proteins with decreased abundance in *A. fumigatus* Δ*gtmA* compared to wild-type following extended culture. Data sorted by fold change, in descending order.

Protein Description	Log_2(Fold Decrease)	Peptides	Seq coverage [%]	Protein IDs
Non-heme Fe(II) and alpha-ketoglutarate-dependent dioxygenase; catalyses the conversion of fumitremorgin B to verruculogen	-4.32466	21	87.3	AFUA_8G00230
Phytanoyl-CoA dioxygenase family protein	-4.17772	12	46.8	AFUA_8G00480
O-methyltransferase, putative	-3.85167	11	70.6	AFUA_8G00390
IgE-binding protein	-3.76683	3	34.5	AFUA_6G00430
Putative methyl transferase; member of the pseurotin A gene cluster; conidia-enriched protein; hypoxia induced protein	-3.28917	28	79.7	AFUA_8G00550
Cysteine-rich secreted protein	-3.27599	15	63.3	AFUA_7G01060
Conserved hypothetical protein, hypoxia induced protein	-3.24847	12	84.7	AFUA_7G01060
DltD N-terminal domain protein (BF Unique)	-3.16375	15	78.4	AFUA_8G00380
Glutathione S-transferase, putative	-2.96915	11	41	AFUA_4G14380
Putative secreted 1,4-beta-D-glucan glucanhydrolase	-2.90284	27	53.3	AFUA_7G06140

Table 3: Proteins encoded by the intertwined secondary metabolite supercluster on chromosome 8 of *A. fumigatus* (AFUA_8G00100-00720) with **decreased** abundance in *A. fumigatus* Δ*gtmA* compared to wild-type grown for 28 days in Czapek-Dox media. Data sorted by fold change, in descending order.

Protein Description	Log_2(Fold Decrease)	Peptides	Seq coverage [%]	Protein IDs
Putative prenyltransferase involved in fumitremorgin B biosynthesis	Absent	16	39.8	AFUA_8G00250
Polyketide synthase (PKS), encoded in the fma (fumagillin) secondary metabolite gene cluster; required for fumagillin biosynthesis	Absent	27	15.4	AFUA_8G00370
Protein of unknown function	Absent	8	18.2	AFUA_8G00630
translation elongation factor eEF-1, gamma subunit, putative	Absent	9	36.7	AFUA_8G00580
Putative brevianamide F prenyltransferase, predicted to convert brevianamide F to tryprostatin B; involved in the biosynthesis of fumitremorgins	Absent	13	32.3	AFUA_8G00210
Putative O-methyltransferase with a predicted role in fumitremorgin B synthesis	Absent	22	68.9	AFUA_8G00200
Non-heme Fe(II) and alpha-ketoglutarate-dependent dioxygenase; catalyses the conversion of fumitremorgin B to verruculogen	-4.32466	21	87.3	AFUA_8G00230
Putative iron-dependent oxygenase; encoded in the fma (fumagillin) secondary metabolite gene cluster	-4.17772	12	46.8	AFUA_8G00480
Predicted O-methyltransferase; encoded in the fma (fumagillin) secondary metabolite gene cluster	-3.85167	11	70.6	AFUA_8G00390
Putative methyl transferase; member of the pseurotin A gene cluster; conidia-enriched protein; hypoxia induced protein	-3.28917	28	79.7	AFUA_8G00550
Hypoxia induced protein; encoded in the fma (fumagillin) secondary metabolite	-3.24847	12	84.7	AFUA_8G00430

gene cluster				
Putative alpha/beta hydrolase; encoded in the fma (fumagillin) secondary metabolite gene cluster	-3.16375	15	78.4	AFUA_8G00380
Protein of unknown function; encoded in the fma (fumagillin) secondary metabolite gene cluster	-2.85247	10	45.1	AFUA_8G00400
Baeyer-Villiger monooxygenase (BVMO); hypoxia induced protein; encoded in the fma (fumagillin) secondary metabolite gene cluster	-2.74114	41	63.4	AFUA_8G00440
Non-ribosomal peptide synthetase (NRPS); PKS/NRPS hybrid; multidomain protein; required for pseurotin A production; transcript induced by voriconazole; induced by hypoxia and in infected mouse lungs	-1.60039	105	36.9	AFUB_086030

igure 1

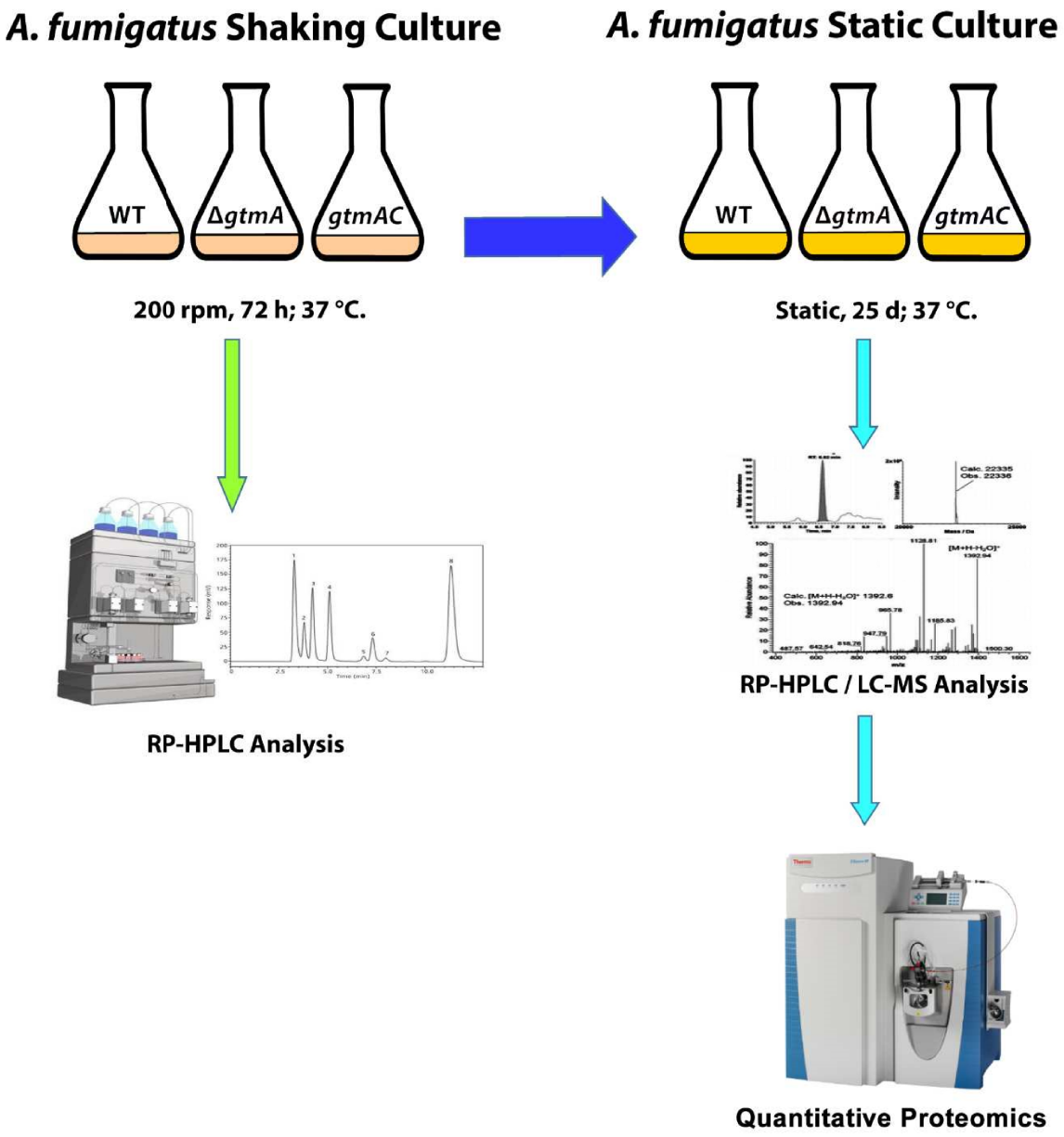
A. fumigatus Shaking Culture
A. fumigatus Static Culture
WT
ΔgtmA
gtmAC
WT
ΔgtmA
gtmAC
200 rpm, 72 h; 37 °C.
Static, 25 d; 37 °C.
RP-HPLC Analysis
RP-HPLC / LC-MS Analysis
Quantitative Proteomics

ure 2

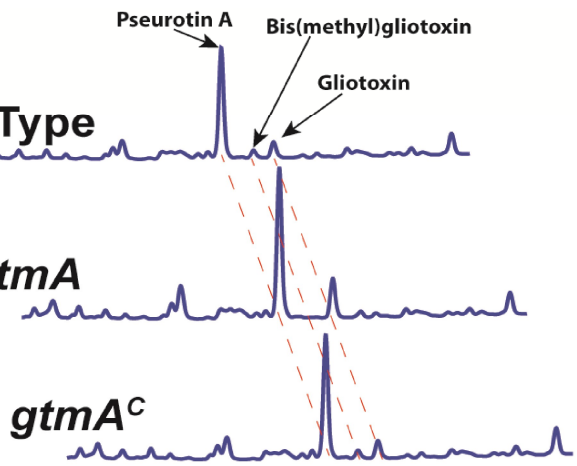
Pseurotin A
Bis(methyl)gliotoxin
Gliotoxin
Type
tmA
gtmA^C

B.

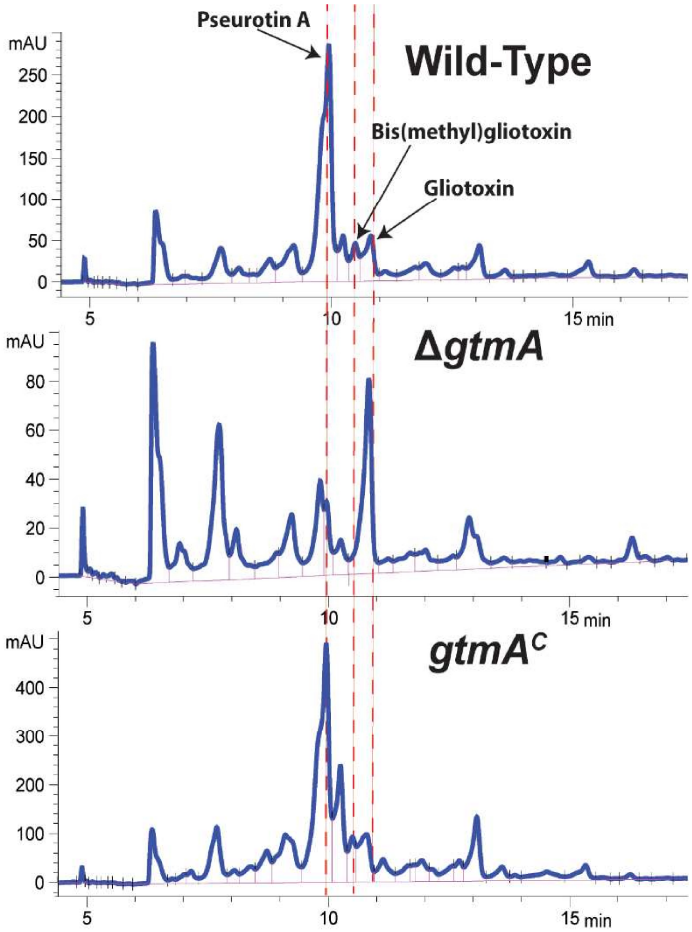
Pseurotin A
Wild-Type
Bis(methyl)gliotoxin
Gliotoxin
mAU
ΔgtmA
gtmA^C
15 min

C.

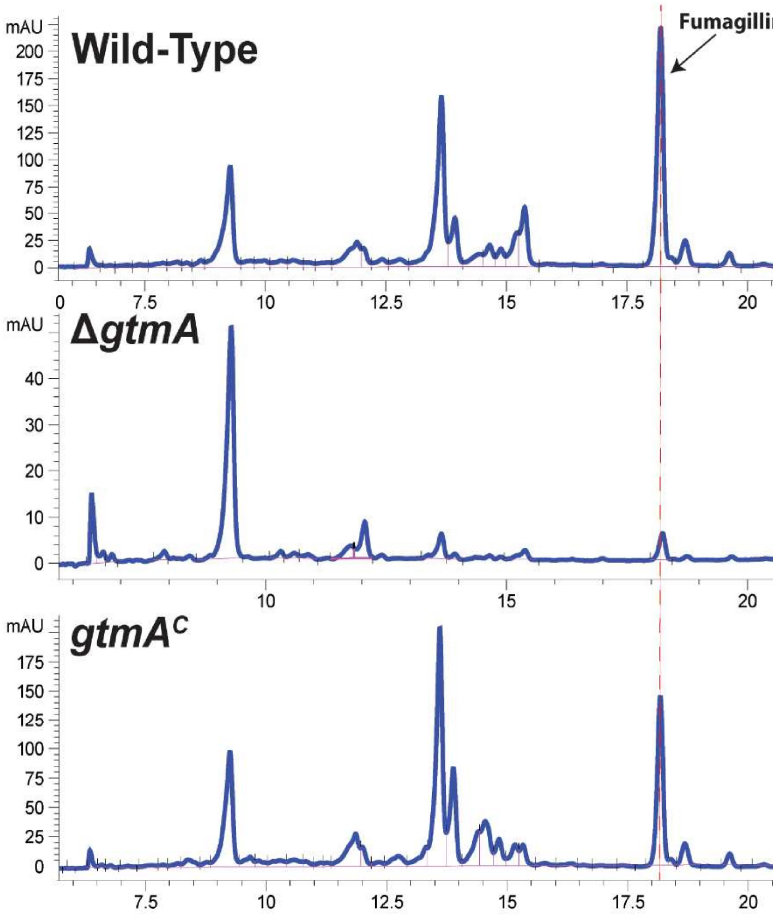
Wild-Type
Fumagilli
mAU
ΔgtmA
gtmA^C

ure 2

D.

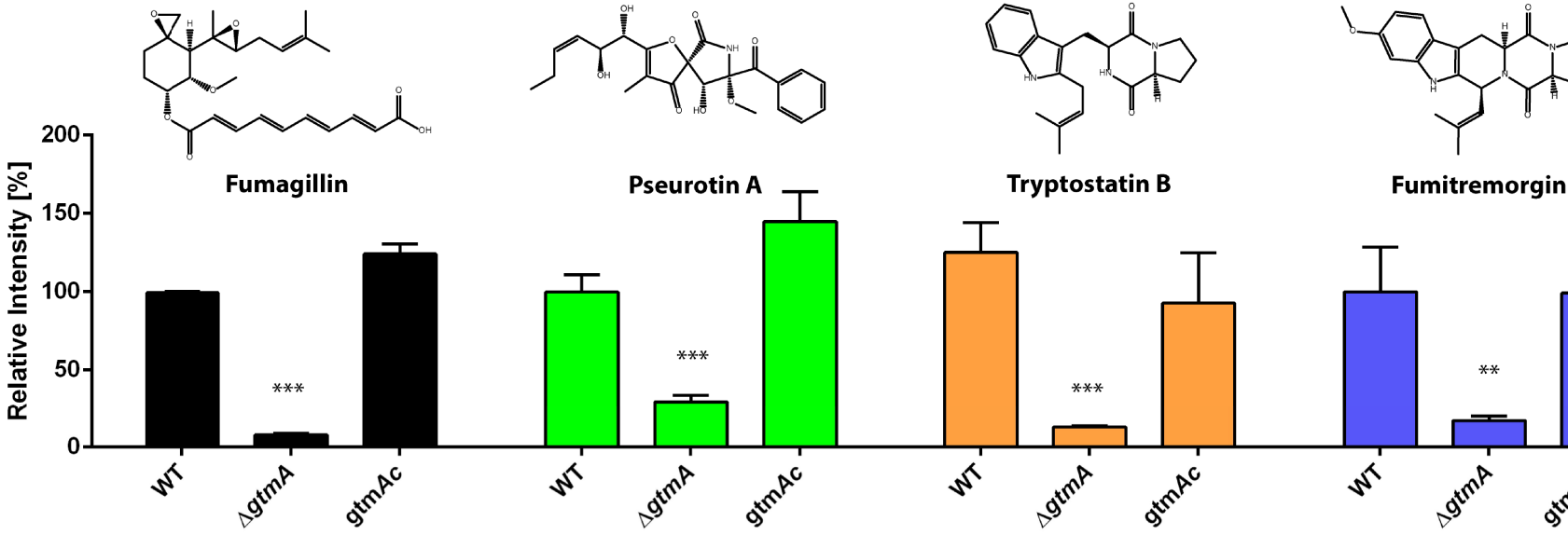
Fumagillin
Pseurotin A
Tryptostatin B
Fumitremorgin
Relative Intensity [%]
200
150
100
50
0
***
***
***
**
WT
ΔgtmA
gtmAc
WT
ΔgtmA
gtmAc
WT
ΔgtmA
gtmAc
WT
ΔgtmA
gtm

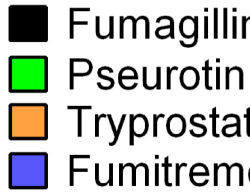
Fumagillin
Pseurotin
Tryprostat
Fumitrem

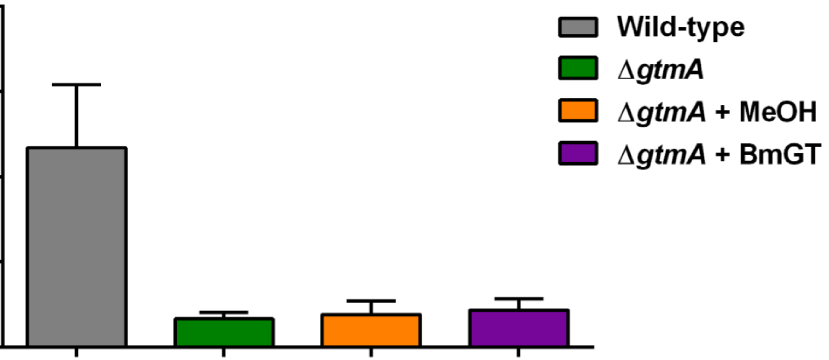
Wild-type
ΔgtmA
ΔgtmA + MeOH
ΔgtmA + BmGT

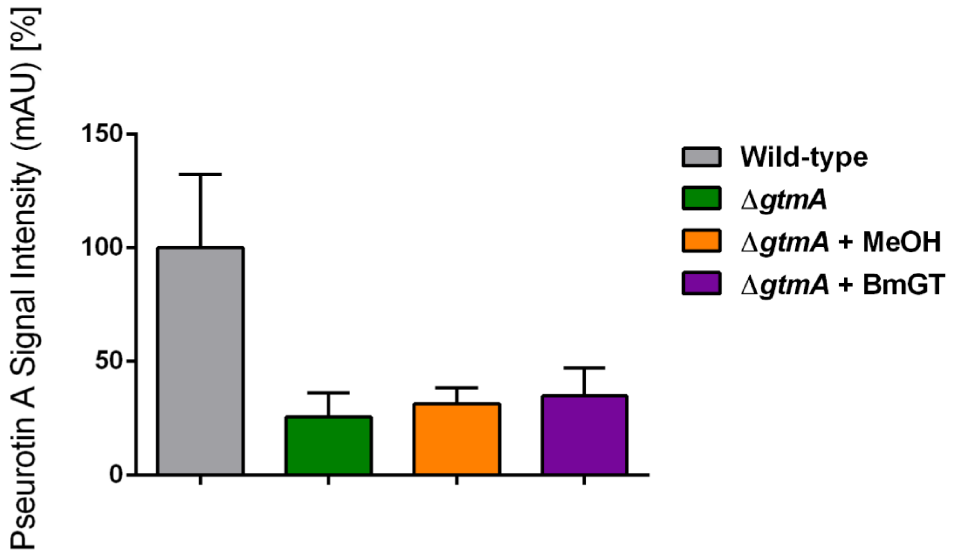
Pseurotin A Signal Intensity (mAU) [%]
150
100
50
0
Wild-type
ΔgtmA
ΔgtmA + MeOH
ΔgtmA + BmGT

ure 3

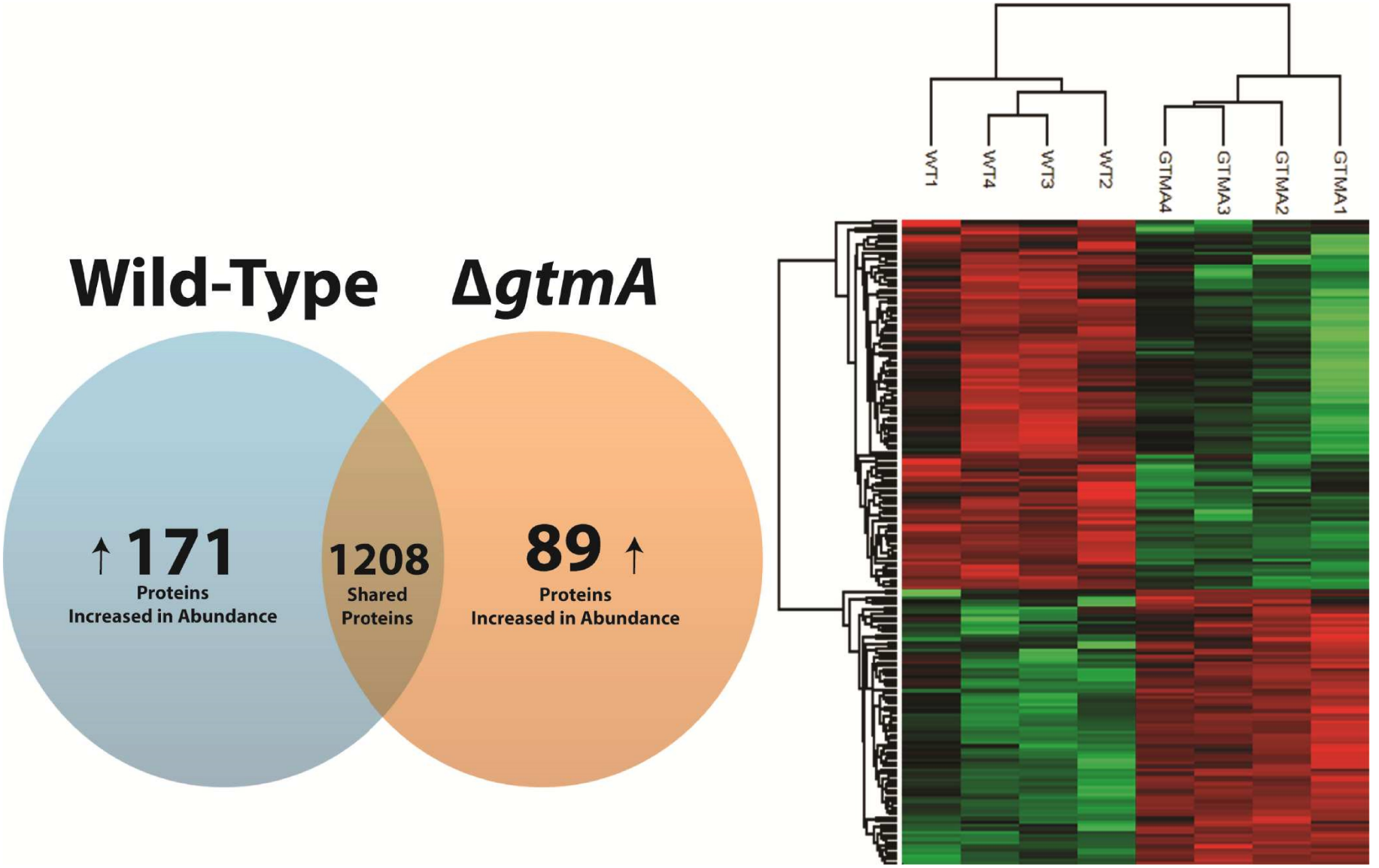
Wild-Type
ΔgtmA
↑ 171
Proteins
Increased in Abundance
1208
Shared
Proteins
89 ↑
Proteins
Increased in Abundance
WT1
WT4
WT3
WT2
GTMA4
GTMA3
GTMA2
GTMA1

ure 4

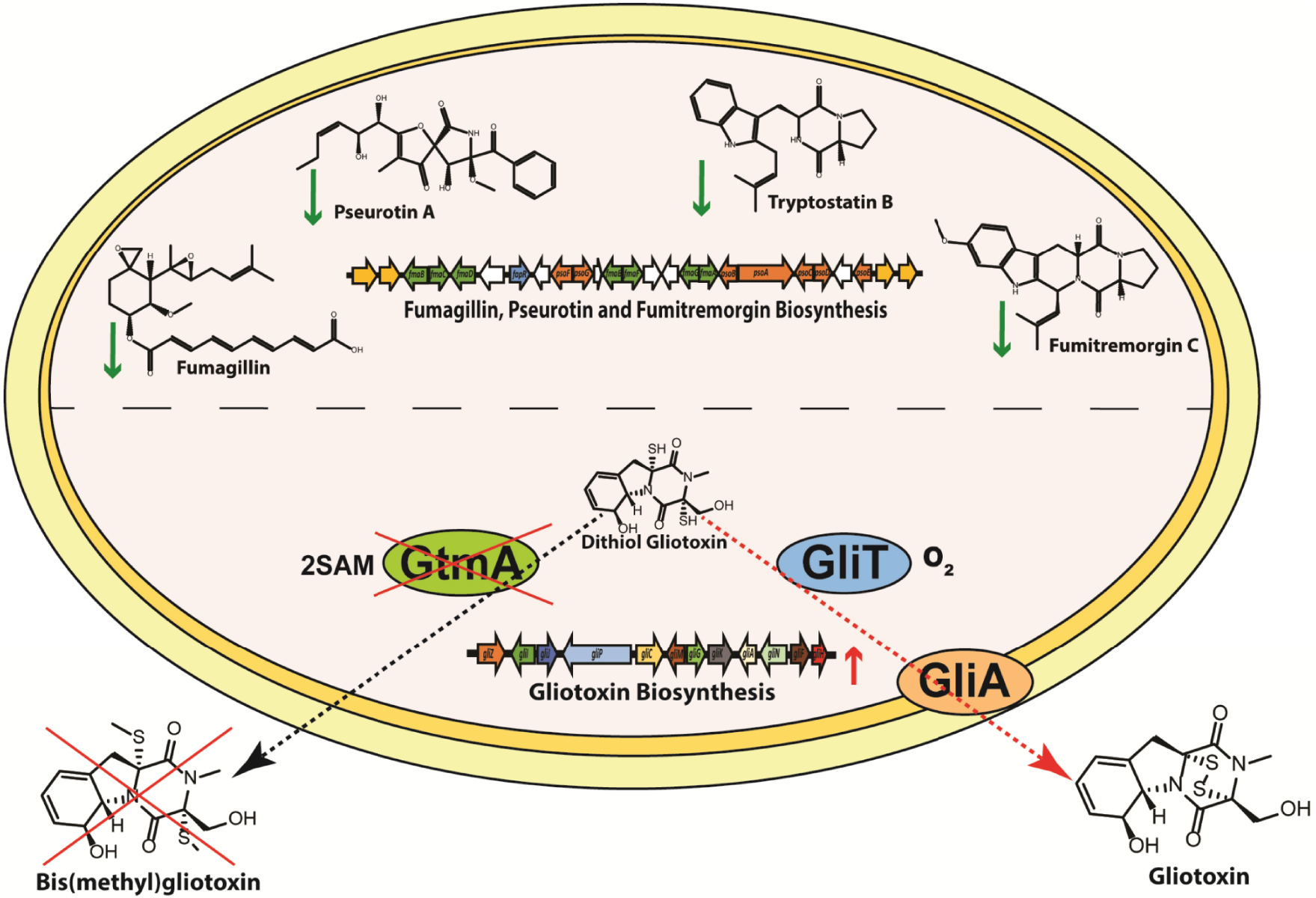
Pseurotin A
Tryptostatin B
Fumagillin
Fumagillin, Pseurotin and Fumitremorgin Biosynthesis
Fumitremorgin C
2SAM
GtmA
Dithiol Gliotoxin
GliT
O_2
Gliotoxin Biosynthesis
GliA
Bis(methyl)gliotoxin
Gliotoxin